Crystal Growth and Substitutional Chemistry of $Pb_2Sr_2MCu_3O_8$

L. F. Schneemeyer,* R. J. Cava, A. C. W. P. James, P. Marsh, T. Siegrist, J. V. Waszczak, J. J. Krajewski, W. P. Peck, Jr., R. L. Opila, S. H. Glarum, J. H. Marshall, R. Hull, and J. M. Bonar

AT&T Bell Laboratories, 600 Mountain Avenue, Murray Hill, New Jersey 07974

Received February 15, 1989

We report the crystal growth and ceramic preparation of $Pb_2Sr_2MCu_3O_8$ phases containing a variety of lanthanoids and lanthanoid/alkaline-earth metal solid solutions. These recently discovered high-temperature superconductors add to our understanding of the chemical and structural features key to superconductivity in cuprates. The growth of millimeter-sized crystals from PbO-rich fluxes is described. Ceramic samples of the $Pb_2Sr_2MCu_3O_8$ phase are formed under low oxygen partial pressures for the majority of the lanthanoids. Systematic structural changes are observed as a function of lanthanoid size. The substitution of alkaline-earth metals on the lanthanoid site and the substitution of barium for strontium to form $Pb_2Ba_2YCu_3O_8$ are also described.

Introduction

The discovery of superconductivity at high temperatures in several structurally distinct cuprate systems including the K_2NiF_4-type La_2CuO_4 phases,[1-3] the perovskite-related $Ba_2YCu_3O_7$ phases,[4,5] and the Aurivillius-related BiSrCaCuO and TlBaCaCuO systems[6-11] has provided insights into chemical and structural features necessary to obtain this fascinating behavior. These materials all contain infinite two-dimensional copper–oxygen sheets as a common structural feature. We recently reported the discovery of a new class of high-temperature superconductors of the formula $Pb_2Sr_2M_{1-x}(AE)_xCu_3O_8$, where M = lanthanoid and AE = Ca or Sr.[12] This new class of cuprates has T_c's as high as 80 K[13] and contains infinite planes of corner-shared CuO_5 pyramids which are present as double layers separated by eight-coordinate lanthanoid ions or a lanthanoid/alkaline-earth metal ion solid solution. Partial substitution of the lanthanoid by the alkaline-earth metal introduces holes into the conducting Cu–O planes, making the system metallic.[14] A unique structural feature, Pb–O/Cu/Pb–O planes containing linearly coordinated Cu(1) atoms similar to those in $Ba_2YCu_3O_6$, separates the copper–oxygen double layers.

While compounds of stoichiometry $Pb_2Sr_2MCu_3O_8$ are not bulk superconductors, as the integral formal oxidation states calculated for the constituent atoms would suggest, the samples become superconducting upon substitution of an alkaline-earth metal on the lanthanoid site. Ceramic studies of the compositional dependence of the superconducting properties of compounds in the series $Pb_2Sr_2Y_{1-x}Ca_xCu_3O_8$ indicated that the optimal composition may have $x \approx 0.5$. The oxidation–reduction behavior of the $Pb_2Sr_2M_{1-x}(AE)_xCU_3O_{8+\delta}$ family of compounds is more complex than that of other high-T_c superconductors,[15] although structural changes and physical properties as a function of δ have not yet been detailed. Like $Ba_2YCu_3O_7$, these $Pb_2Sr_2M_{1-x}(AE)_xCu_3O_8$ phases have a rich substitutional chemistry. For example, silver can partially substitute for the linearly coordinated Cu(1) atoms,[16] and the phase can be formed for the majority of the lanthanoids, including cerium. In this paper, we report details of the preparation of these phases for a variety of lanthanoid constitutents as both ceramics and single crystals. Millimeter-sized crystals suitable for a variety of studies of physical properties are obtained from PbO eutectic melts. The $Pb_2Sr_2MCu_3O_8$ phase is formed under low oxygen partial pressures for the majority of the lanthanoids. Systematic structural changes are observed as a function of lanthanoid size. The substitution of alkaline-earth metals on the lanthanoid site and the substitution of barium for strontium to form $Pb_2Ba_2YCu_3O_8$ are also described.

Experimental Section

Single-crystal samples were analyzed by using X-ray energy dispersive analysis (EDX). Single-phase ceramic samples were used as standards. Samples were mounted on graphite stubs by using graphite-based conducting paint and were examined in a Physical Electronics Model 595 scanning Auger microprobe with a Tracor Northern Model 5400 X-ray detector. The excitation

(1) Bednorz, J. G.; Muller, K. A., *Z. Phys.* **1986**, *B64*, 189.
(2) Takagi, G.; Uchida, S.; Kitazawa, K.; Tanaka, S. Jpn. *J. Appl. Phys.* **1987**, *26*, L231.
(3) Cava, R. J.; van Dover, R. B.; Batlogg, B.; Rietman, E. A. *Phys. Rev. Lett.* **1987**, *58*, 408.
(4) Wu, M. K.; Ashburn, J. R.; Torng, C. J.; Hor, P. H.; Meng, R. L.; Gao, L.; Huang, Z. J.; Wang, Y. O.; Chu, C. W. *Phys. Rev. Lett.* **1987**, *58*, 908.
(5) Cava, R. J.; Batlogg, B.; van Dover, R. B. van Dover; Murphy, D. W.; Sunshine, S.; Siegrist, T.; Remeika, J. P.; Rietman, E. A.; Zahurak, S.; Espinosa, G. P. *Phys. Rev. Lett.* **1987**, *58*, 1676.
(6) Maeda, H.; Tanaka, Y.; Fukutomi, M.; Asano, T. *Jpn. J. Appl. Phys.* **1988**, *27*, L209.
(7) Sunshine, S. A.; Siegrist, T.; Schneemeyer, L. F.; Murphy, D. W.; Cava, R. J.; Batlogg, B. van Dover, R. B.; Fleming, R. M.; Glarum, S. H.; Nakahara, S.; Farrow, R.; Krajewski, J. J.; Zahurak, S. M.; Waszczak, J. V.; Marshall, J. H.; Marsh, P.; Rupp, L. W.; Peck, W. F. *Phys. Rev. B* **1988**, *38*, 893.
(8) Tarascon, J. M.; LePage, Y.; Barboux, P.; Bagley, B. G.; Greene, L. H.; McKinnon, W. R.; Hull, G. W.; Giroud, M.; Hwang, D. M. *Phys. Rev. B* **1988**, *38*, 896.
(9) Subramanian, M. A.; Torardi, C. C.; Calabrese, J. C.; Gopalakrishnan, J.; Morrissey, K. J.; Askew, T. R.; Flippen, R. B.; Chowdhry, U.; Sleight, A. W. *Science* **1988**, *239*, 1015.
(10) Sheng, Z. Z.; Hermann, A. M. *Nature* **1988**, *332*, 138.
(11) Subramanian, M. A.; Calabrese, J. C.; Torardi, C. C.; Gopalakrishnan, J.; Askew, T. R.; Flippen, R. B.; Morrissey, K. J.; Chowdhry, U.; Sleight, A. W. *Nature* **1988**, *332*, 420.
(12) Cava, R. J.; Batlogg, B.; Krajewski, J. J.; Rupp, L. W.; Schneemeyer, L. F.; Siegrist, T.; van Dover, R. B.; Marsh, P.; Peck, W. F.; Gallagher, P. K.; Glarum, S. H.; Marshall, J. H.; Farrow, R. C.; Waszczak, J. V.; Hull, R.; Trevor, P. *Nature* **1988**, *336*, 221.
(13) Subramanian, M. A.; Gopalakrishnan, J.; Torardi, C. C.; Gai, P. L.; Boyes, E. D.; Askew, T. R.; Flippen, R. B.; Farneth, W. E.; Sleight, A. W. *Physica C* **1989**, *157*, 124.
(14) Mattheiss, L. F.; Hamann, D. R. *Phys. Rev.*, in press.
(15) Gallagher, P. K.; O'Bryan, H. M.; Cava, R. J.; James, A. C. W. P.; Murphy, D. W.; Rhodes, W. W.; Krajewski, J. J.; Peck, W. F.; Waszczak, J. V. *Chem. Mater.* **1989**, *1*, 277.
(16) James, A. C. W. P.; Murphy, D. W. *Chem. Mater.* **1989**, *1*, 169.

0897-4756/89/2801-0548$01.50/0 © 1989 American Chemical Society

Table I. Crystal Growth Parameters

precursor composition	wt % PbO	T_{max}, °C	soak time, h	cooling rate, °C/h	comments
$Sr_3YCu_4O_x$	50	1025	0.5	20	
$Sr_3YCu_4O_x$	50	1000	0.5	20	less melting, few crystals
$Sr_3YCu_4O_x$	50	1025	0.5	5	larger crystals
$Sr_3Y_{0.75}Ca_{0.25}Cu_4O_x$	50	1025	0.5	20	little Ca incorp
$Sr_3YCu_4O_x$	75	1025	0.5	20	less and smaller crystals
$Sr_3Y_{0.5}Cu_4O_x$	50	1025	0.5	20	less crystals
$Sr_2CaYCu_4O_x$	50	1025	0.5	20	Ca on the Y site

source was a 20-keV 10-nA electron beam.

Lattice structure images were taken by using the phase-contrast technique with a point-to-point resolution of ≈2 Å. A JEOL 4000EX transmission electron microscope operated at 200 keV was used for these studies. The image is recorded under experimental operating conditions (Scherzer defocus, very thin specimen) where the image intensity closely represents the projected crystal potential.

Materials Synthesis

Crystal Growth. Bulk single crystals are useful for a variety of measurements of physical properties including anisotropic behavior and structural characterization studies. Like most complex materials, the $Pb_2Sr_2MCu_3O_8$-related phases do not melt congruently. Thus, a high-temperature solution approach is useful for the growth of bulk crystals. Flux growth, including eutectic melt growth techniques, has been used for the preparation of crystals of other cuprate superconductors.[17] Crystals of the $Pb_2Sr_2M_{1-x}(AE)_xCu_3O_8$ phases may be grown from PbO melts.

Lead oxide is a classic flux for the growth of oxides[18] including various ferrites, garnets, and spinels, as well as La_2CuO_4.[19] It has a relatively low melting point (886 °C) and a high solubility for a variety of refractory oxides. In this case, lead is a constituent of the desired phase; thus contamination of the resulting crystals by the flux is not a concern. Lead oxide is, however, relatively volatile and highly toxic, and appropriate precautions were taken in its handling.

As in the case of ceramic samples, a precursor technique was used for crystal growth. Precursors containing the alkaline-earth metal, lanthanoid, and copper constituents in desired ratios were prepared from appropriate oxides, carbonates, or nitrates by using standard ceramic techniques, including firing at 850 °C with an intermediate grinding step to ensure adequate mixing. These precursors were then combined with lead oxide in a 1:1 weight ratio, placed in a high-density alumina crucible, and heat-treated under low oxygen partial pressure conditions, typically in flowing 1% O_2. In higher O_2 partial pressures, e.g., air, a nonsuperconducting triple perovskite phase of composition $Sr_2MCu_{3-x}Pb_xO_{7-\delta}$ was obtained as an intergrowth. No aluminum from the crucible could be detected in the crystals.

In a typical experiment, samples were heated rapidly to 1025 °C, soaked at 1025 °C for 30 min, then cooled at 2 °C/min to temperatures between 800 and 400 °C, and finally rapidly cooled to room temperature. Experimental parameters including precursor composition, cooling rate, and solute concentration are summarized in Table I. Yttrium-containing samples are used as representative examples. Only a small number of the relevant growth parameters have been varied so far. As is typical in crystal growth, slower cooling rates favored larger crystals. Crystals with dimensions 1 × 1 × 0.1 mm^3 were routinely obtained. Crystals were grown for all the lanthanoids (except scandium) by using similar melt compositions and growth conditions. Larger lanthanoids such as neodymium yielded larger crystals.

Crystal growth in this system is very reminiscent of the growth of $Ba_2YCu_3O_7$ crystals from CuO-rich melts.[20] The mixtures used here also only partially melt at the temperatures examined. Crystals grow as flat platelets at the edges of the hardened charge and are often free-standing, simplifying problems of separating the crystals from residual flux. Other, more blocky crystals are found embedded in the hardened charge. Crystals have an unusual morphology as illustrated in Figure 1 for crystals of stoichiometry $Pb_2Sr_2Dy_{1-x}Ca_xCu_3O_8$, $x \approx 0.3$. The facets along the edges of the plates probably indicate that the crystals are twinned. Although crystallographic studies have treated these phases as orthorhombic, the crystal habit indicates that the true crystal symmetry may be lower, such as monoclinic or even triclinic, although deviations from orthorhombic symmetry are probably small. Examination of regions of flux adhering to the crystals using a scanning electron microscope with energy dispersive spectroscopy indicates that the flux is PbO.

Like their ceramic counterparts, the single crystals have large variations in oxygen contents.[15] Crystals display a range of T_c's depending on thermal treatment following the growth portion of a given run. For a given set of growth parameters, behavior is reproducible. We are continuing to investigate the relationship between T_c and δ for $Pb_2Sr_2M_{1-x}AE_xCu_3O_{8+\delta}$ phases.

Lanthanoid Substitutions. We have prepared ceramic samples of the parent $Pb_2Sr_2MCu_3O_8$ phases containing the various trivalent lanthanoid ions. The lanthanoid ion occupies the site between the Cu–O planes as seen in Figure 2. We find that, with the exception of the very small Sc^{3+} ion (r = 0.87 Å), this phase forms for all lanthanoid ions.

Ceramic $Pb_2Sr_2MCu_3O_8$ samples were prepared by using the precursor technique as described earlier.[12] An intimate stoichiometric mixture of PbO and the appropriate prereacted ceramic precursor ($Sr_2MCu_3O_x$) are pressed into a pellet and then reacted at 860 °C for several hours in a flowing stream of 1% O_2 in N_2. Careful control of the oxygen partial pressure is required to avoid the formation of 123-type $Sr_2M(Cu,Pb)_3O_x$ impurity phases. The 1% O_2 atmosphere is apparently sufficiently reducing to allow Ce, Pr, and Tb to behave as +3 ions. This contrasts with the behavior observed for lanthanoid ions with readily accessible +4 states under the more oxidizing conditions (reactions carried out in air or O_2) typically employed in the synthesis of 123-type phases. Under these conditions, Tb and Ce act as +4 ions, forming $BaMO_3$ perovskite phases.[21]

(17) Schneemeyer, L. F. *AACG Newsletter* **1988**, *18*, 3.
(18) Elwell, D.; Scheel, H. J. *Crystal Growth from High-Temperature Solutions*; Academic Press: New York, 1975.
(19) Espinosa, G. P.; Cooper, A. S.; Remeika, J. P. Private Communication.
(20) Schneemeyer, L. F.; Waszczak, J. V.; Siegrist, T.; van Dover, R. B.; Rupp, L. W.; Batlogg, B.; Cava, R. J.; Murphy, D. W. *Nature* **1987**, *332*, 601.
(21) Schneemeyer, L. F.; Waszczak, J. V.; Zahurak, S. M.; van Dover, R. B.; Siegrist, T. *Mater. Res. Bull.* **1987**, *22*, 1467.

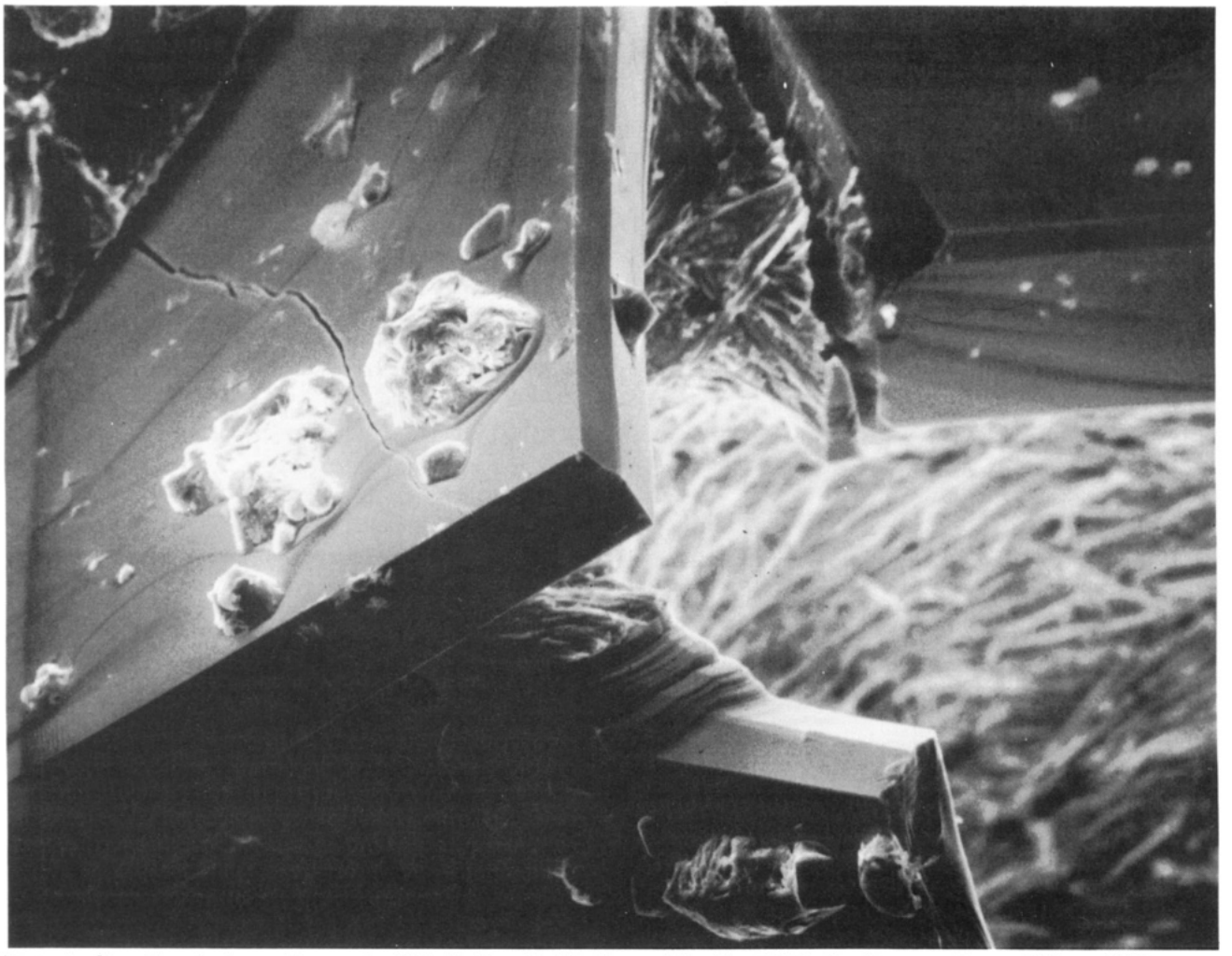

Figure 1. Scanning electron micrograph of $Pb_2Sr_2Dy_{1-x}Ca_xCu_3O_8$ crystals. Crystals in the foreground are ≈100 μm thick.

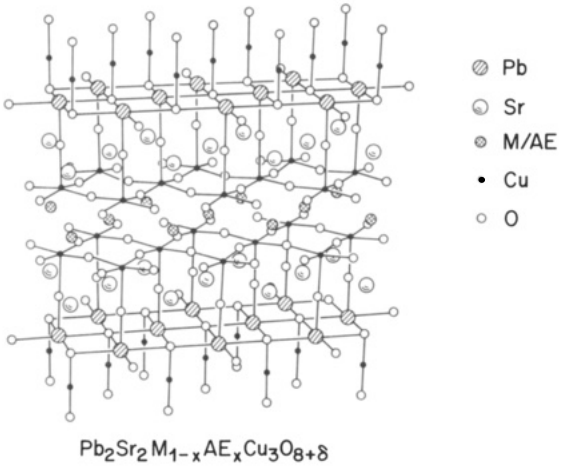

Figure 2. Extended lattice view of the structure of $Pb_2Sr_2MCu_3O_8$.

The powder patterns for the $Pb_2Sr_2MCu_3O_8$ samples are consistent with a c-centered orthorhomic cell that is based on a multiple-layer perovskite. Crystallographic data as a function of the lanthanoid constituent are listed in Table II. The unit cell parameters, a, b, and c as well as the unit-cell volume all increase with increasing lanthanoid ionic radius as shown in Figures 3 and 4. The data show some scatter which are within the standard deviations of the measurements or may result from subtle variations in oxygen stoichiometries for different preparations. The majority of the samples were single phase by powder X-ray diffraction, although the sample that shows the greatest deviations, M = Ce, showed small traces of an impurity phase, at the level of a few percent, in its X-ray pattern.

Table II. Crystallographic Data for $Pb_2Sr_2MCu_3O_8$

M	a, Å	b, Å	c, Å	V,[a] Å^3	R_I[28], Å
Y	5.394 (1)	5.430 (1)	15.731 (4)	460.8	0.90
La	5.457 (2)	5.495 (2)	15.886 (6)	476.4	1.03
Ce	5.429 (2)	5.474 (2)	15.827 (6)	470.4	1.01
Pr	5.447 (3)	5.481 (3)	15.814 (9)	472.1	0.99
Nd	5.442 (2)	5.477 (2)	15.822 (6)	471.6	0.983
Sm	5.424 (2)	5.459 (2)	15.772 (6)	466.6	0.958
Eu	5.423 (2)	5.461 (2)	15.789 (7)	467.6	0.947
Gd	5.412 (3)	5.445 (3)	15.732 (8)	463.6	0.938
Tb	5.411 (3)	5.451 (3)	15.751 (9)	464.6	0.923
Dy	5.403 (3)	5.441 (3)	15.734 (8)	462.5	0.912
Ho	5.398 (2)	5.435 (2)	15.748 (6)	462.0	0.901
Er	5.393 (2)	5.430 (2)	15.729 (5)	460.6	0.89
Tm	5.384 (2)	5.422 (2)	15.729 (7)	459.1	0.88
Yb	5.381 (2)	5.414 (2)	15.727 (6)	458.2	0.868
Lu	5.381 (2)	5.420 (2)	15.756 (6)	459.3	0.86

[a] Standard deviation is ±0.5 Å^3.

Small amounts of superconductivity (1% or less) are often observed in samples of composition $Pb_2Sr_2MCu_3O_8$, where formal valencies have integral values, due, perhaps, to variations in the oxygen content or to inhomogeneities in the Sr:M ratio. Partial substitution of calcium on the lanthanoid site produces bulk superconductivity with T_c's above 70 K for ceramic samples prepared in 1% O_2 for all of the lanthanoids except cerium. For example, $Pb_2Sr_2YB_{0.625}Ca_{0.375}Cu_3O_{8+\delta}$ has a T_c of 70 K. Because the dependence of T_c on δ is not known, we were unable to

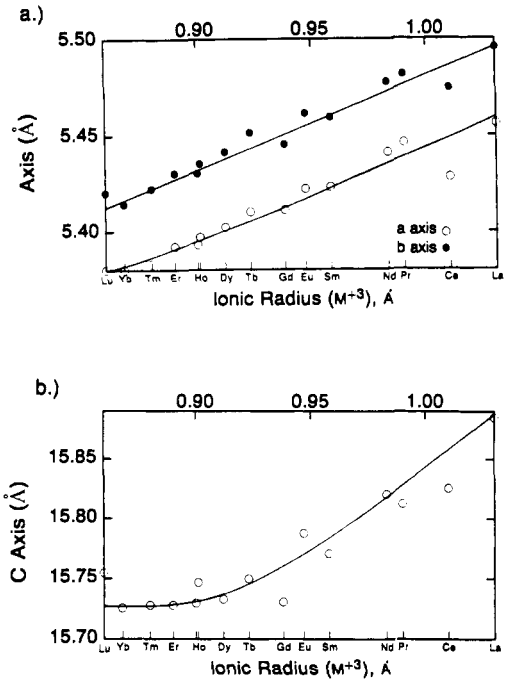

Figure 3. Variation of lattice parameters with lanthanoid ionic radius.

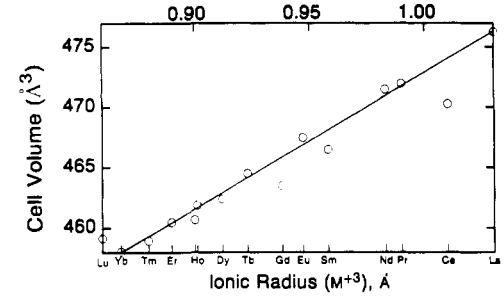

Figure 4. Variation of unit-cell volume with lanthanoid ionic radius.

determine whether the lanthanoid size causes any systematic shift in T_c.

While $Ba_2PrCu_3O_7$ forms as a tripled perovskite, this compound has not been found to superconduct. This result has been attributed to the greater lateral extent of the f electrons in Pr relative to the other lanthanoids resulting in alterations in the band structure.[22] However, the praseodymium-containing phase in this system, $Pb_2Sr_2Pr_{1-x}(AE)_xCu_3O_8$, is a high-temperature superconductor, while the $Pb_2Sr_2Ce_{1-x}(AE)_xCu_3O_8$ compounds are isostructural with the superconducting phases but are not superconducting for any alkaline-earth metal doping level. In cerium, the f orbitals are the most extended of any of the rare-earth metals. Further study of compounds in the $Pb_2Sr_2Ce_{1-x}Ca_xCu_3O_8$ system may shed additional light on the role of f-orbital interactions on superconductivity in cuprates.

Alkaline-Earth Metal Substitutions. As discussed above, compounds of stoichiometry $Pb_2Sr_2MCu_3O_8$ are not bulk superconductors, but upon substitution of calcium at the lanthanoid site, the samples become superconducting. Structural studies[12] indicate that strontium also substitutes on the lanthanoid site in samples prepared from strontium-rich precursors such as $Sr_3MCu_4O_x$, listed in Table I. Indeed, these crystals are superconducting with reasonable Meissner fractions (>20%) and sharp resistive transitions. However, attempts to incorporate strontium in ceramic preparations have not been successful. While the coordination geometry of the lanthanoid site is suitable for calcium, strontium typically prefers a larger coordination site. We have used energy dispersive X-ray analysis (EDX) to study the single-crystal samples. Results are consistent with a stoichiometry of $Pb_2Sr_{2+x}M_{1-x}Cu_3O_8$, $x \approx 0.2$ in the single-crystal samples, similar to the composition determined in single-crystal structural determinations as described later in this paper.

Partial substitution of calcium on the strontium site has also been studied in ceramic samples. The lanthanoid site has a size and coordination geometry that is suitable for Ca^{2+}. The solubility limit is near $x = 0.25$ for samples in the series $Pb_2Sr_{2-x}Ca_xY_{0.5}Ca_{0.5}Cu_3O_8$, which are superconductors. A T_c of 77 K was measured for a sample of composition $Pb_2Sr_{1.75}Ca_{0.25}Y_{0.5}Ca_{0.5}Cu_3O_8$.

$Pb_2Ba_2YCu_3O_8$. In addition to partial calcium substitution on the alkaline-earth metal site, we have also prepared the barium analogue of $Pb_2Sr_2MCu_3O_8$ using a precursor technique similar to the one described above. Powder X-ray diffraction indicates an orthorhombic cell that is based on a multiple layer perovskite isomorphous with $Pb_2Sr_2MCu_3O_8$. The c axis is elongated due to the larger size of barium, which replaces strontium in an interlayer site, while the a and b axes are increased only slightly. The characteristic powder pattern for this analogue is given in Table III. The apparent symmetry is orthorhombic, with lattice parameters $a = 5.471$ (2) Å, $b = 5.504$ (2) Å, and $c = 16.195$ (5) Å.

We have been unable to substitute calcium on the lanthanoid site in this barium analogue, and thus this phase

Table III. Powder Diffraction Pattern for $Pb_2Ba_2YCu_3O_8$, $a = 5.471$ (2), $b = 5.504$ (2), $c = 16.195$ (5) Å

h	k	l	$2\theta^a$	d	$I/I_0 \times 100\%$
0	0	4	21.90	4.058	4.5
1	1	1	23.52	3.783	21.7
1	1	2	25.40	3.507	8.6
0	0	5	27.52	3.241	15.7
1	1	3	28.29	3.154	14.8
1	1	4	31.91	2.805	100.0
0	2	0	32.51	2.754	39.9
2	0	0	32.69	2.739	40.3
2	0	1	33.16	2.701	13.2
0	0	7	38.89	2.316	6.5
1	1	6	40.67	2.203	11.7
0	2	5	43.10	2.099	16.8
2	0	5	43.28	2.091	10.3
0	0	8	44.74	2.025	10.0
2	2	0	46.78	1.942	37.9
2	2	1	47.19	1.926	4.2
0	2	7	51.59	1.772	3.8
2	0	7			
1	3	1	52.88	1.731	4.8
3	1	1	53.16	1.723	4.1
2	2	5	55.09	1.667	7.9
0	2	8	56.36	1.632	19.3
0	0	10	56.83	1.620	5.7
1	3	4	57.66	1.599	24.8
3	1	4	57.91	1.592	20.2
2	2	6	58.55	1.576	4.2
2	2	7	62.41	1.488	4.6
1	3	6	63.57	1.463	3.6
3	1	6	63.79	1.459	3.6
2	2	8	66.74	1.401	6.4
0	2	10	67.05	1.396	7.4
2	0	10			
0	4	0	68.10	1.377	6.6
4	0	0	68.57	1.369	5.1

[a] Measured by using Cu Kα radiation.

(22) Solderholm, L.; Zhang, K.; Hinks, D. G.; Beno, M. A.; Jorgensen, J. D.; Segre, C. U.; Schuller, I. K. *Nature* 1987, *328*, 604.

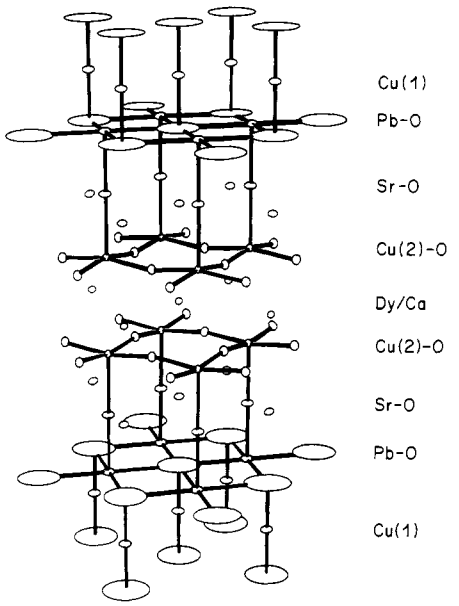

Figure 5. Unit-cell plot showing the atom connectivity in $Pb_2Sr_2MCu_3O_8$. Of interest are the oblate thermal parameters of the oxygens in the PbO planes.

is not superconducting. Instead, under conditions examined so far, the $BaPbO_3$-related perovskite phase is produced when calcium is added.

Structural Studies

X-ray Studies of $Pb_2Sr_2MCu_3O_8$. While preliminary results of X-ray structural studies have been reported for $Pb_2Sr_2MCu_3O_8$,[12] we describe these studies in detail here. Also, we examine the question of the structural basis for the orthorhombicity in $Pb_2Sr_2MCu_3O_8$. The metal atom sublattice, which dominates the scattering in the X-ray diffraction experiment, is pseudotetragonal. Thus, the oxygen atom positions must determine the true crystal symmetry of this material, which must be orthorhombic or lower. However, oxygen contributes only about 1% to the total X-ray scattering. Neutron powder profile analysis, which is more sensitive to oxygen, has been carried out on a ceramic sample of stoichiometry $Pb_2Sr_2YCu_3O_8$.[23] Results of this study indicate that the orthorhombic distortion is caused by disordering about the general position of the oxygens of the PbO layers in the *ab* plane. Also, electron microscopy indicates that crystals are twinned on the (110) planes, a twinning plane 45° to that found in $Ba_2YCu_3O_7$.[24] These studies indicate that the unit cell induced by the small oxygen atom displacements is well-ordered and not c centered.

We have reexamined our single-crystal X-ray data[12] in light of the above results. In general, crystal quality was a concern because of the (110) twinning and the large mosaic spreads seen in most of the crystals. We therefore studied crystals from four different preparations containign varying lanthanoid/alkaline-earth metal combinations. A crystal of composition $Pb_2Sr_{2+x}Nd_{1-x}Cu_3O_{8\pm\delta}$ was most thoroughly investigated, and data from this crystal are given in this paper. Unfortunately, our attempts to deconvolve the twinning by refining a twinning parameter were unsuccessful as all models we explored diverged. However, the thermal parameters of the oxygen atom O3 indicate disorder. A plot of the unit cell with thermal ellipsoids at 50% of the probability density function is shown in Figure 5. This thermal ellipsoid is prolate with large amplitudes of vibration in the *ab* plane suggesting rotation about the copper atom. Indeed, shifts in the oxygen positions in the Pb–O plane lead to the orthorhombic distortions in this phase. We also note that no distortions of the lanthanoid coordination sphere are seen despite partial occupancy of the site by strontium. As pointed out earlier, strontium typically prefers a larger site than calcium or lanthanoids. Finally, while additional oxygen is known to be incorporated in the structure following certain thermal treatments,[15] we have seen no significant excess electron density due to such oxygen in the samples studied so far.

Results from X-ray diffraction studies are summarized in Table IV. Lattice parameters are given in the orthorhombic setting, space group *Cmmm*. Alkaline-earth metal substitutional-doping levels on the lanthanoid site were deduced from the calculated electron density at that site. In the case where calcium was present in the crystal, all of the change in electron density from that expected for the lanthanoid was attributed to the presence of calcium. Of course, it is possible that the site is simultaneously shared by a mixture of lanthanoid, calcium, and strontium ions. Table IV also gives typical bond lengths and angles. Atom positional parameters and thermal parameters for the $Pb_2Sr_{2+x}Nd_{1-x}Cu_3O_8$ sample are listed in Table V. A summary of the data aquisition parameters used for this sample is given in Table VI.

Homologous Series. It is interesting to ask whether additional structurally related phases, in addition to the isomorphous series of lanthanoid-containing phases and solid solutions between the alkaline-earth metal and lan-

Table IV. X-ray Structural Data for $Pb_2Sr_2M_{1-x-y}Sr_xCa_yCu_3O_8$ Phase

M/AE	x/y	a, Å	b, Å	c, Å
Dy/Sr	x = 0.237 (8)	5.404 (1)	5.423 (1)	15.819 (6)
Dy/Ca	y = 0.416 (8)	5.380 (1)	5.399 (1)	15.746 (7)
Nd/Sr	x = 0.234 (12)	5.432 (1)	5.4510 (9)	15.797 (7)
Tm/Sr	x = 0.427 (4)	5.389 (1)	5.408 (1)	15.808 (6)

	bond	length, Å	bond	angle, deg
[2]	Cu(1)–O	1.769 (17)	O–Cu(1)–O	180
[1]	Pb–O	2.142 (12)	O–Pb–O (out-of-plane)	89.6 (4)
[4]	Pb–O	2.6967 (1)	O–Pb–O (in-plane)	179.3 (7)
[1]	Sr–O	2.609 (17)		
[4]	Sr–O	2.728 (6)		
[2]	Sr–O	2.740 (2)		
[2]	Sr–O	2.758 (2)		
[1]	Cu(2)–O	2.228 (12)	O–Cu–O (out-of-plane)	96.0 (2)
[4]	Cu(2)–O	1.924 (1)	O–Cu–O (in-plane)	89.0 (1)
				89.8 (1)
[8]	Nd/Sr–O	2.458 (5)		

Table V. X-ray Structural Data for $Pb_2Sr_2Nd_{1-x}Ca_xCu_3O_8$[a] (Pseudotetragonal *P4/mmm*)

	x	y	z	u_{11}	u_{33}[b]
Cu(1)	0	0	0	0.0185 (16)	0.0068 (9)
Pb	1/2	1/2	0.11141 (3)	0.0716 (3)	0.0043 (2)
Sr	0	0	0.27834 (7)	0.0100 (6)	0.0043 (5)
Cu(2)	1/2	1/2	0.38925 (11)	0.0059 (7)	0.0063 (7)
Nd/Sr[c]	0	0	1/2	0.0067 (6)	0.0038 (4)
O(1)	1/2	1/2	0.24655 (53)	0.0178 (43)	0.0042 (32)
O(2)	0	1/2	0.40161 (36)	0.0105 (27)	0.0134 (25)
O(3)	0	0	0.11276 (78)	0.23570 (372)	0.0113 (55)

[a] The cell is treated as tetragonal (*P4/mmm*) with a 3.8510 (5) Å, c = 15.797 (3) Å, ratrher than the fully twinned *Cmmm* setting. [b] Thermal parameters are expressed in Å^2. [c] Mixed occupancy site Nd occupancy = 81.6 (6)%, Sr occupany = 18.4 (6)%.

(23) Cava, R. J.; Marezio, M.; Krajewski, J. J.; Peck, W. F.; Santoro, A.; F. Beech, F. *Physica C* **1989**, *157*, 272.
(24) Hewat, E. A.; Capponi, J. J.; Cava, R. J.; Chaillout, C.; Marezio, M.; Tholence, T. L. *Physica C*, in press.

Table VI. Summary of Data Aquisition Parameters for $Pb_2Sr_{2+x}Nd_{1-x}Cu_3O_{8\pm\delta}$

space group	$P4/mmm$
a, Å	3.8510 (5)
c, Å	15.797 (3)
vol Å^3	234.2 (1)
Z	2
x	0.184 (6)
cryst vol, mm^3	0.105 × 0.095 × 0.015
cryst shape	platelet
ρ_{calc}, g cm^{-3}	7.47
linear abs coeff, mm^{-1}	59.3
scan type	ω–2θ
max λ^{-1} sin θ, Å^{-1}	0.9
radiation (graphite monochromator)	Mo Kα
data coll	4791
unique data	511
data with $F_o > 3\sigma F_o$	257
no. of variables	24
$R(F)$	0.0252
$R(F_w)$	0.0257

thanoid constituents, exist in this system. The BiSrCaCuO and TlBaCaCuO systems belong to a homologous series with the general formula $M_2AE_2Ca_{n-1}Cu_nO_{2n+\delta}$ in which varying numbers of $CaCuO_2$ layers are added to the structure, raising T_c (at small n). High-resolution electron microscopy studies of bismuth or thallium alkaline-earth metal cuprates show that intergrowth, the insertion of these additional $CaCuO_2$ layers, is a typical feature of these phases.[25] In these new $Pb_2Sr_2MCu_3O_8$ phases, we might imagine a series of compounds of general formula $Pb_2Sr_2M_{1-x}Ca_{n+x}Cu_{3+n}O_{8+2n}$. However, all attempts to synthesize additional members in this series have been unsuccessful so far. In $Pb_2Sr_2MCu_3O_8$, in contrast to the bismuth or thallium alkaline-earth metal cuprates, TEM studies show samples to be remarkably free from stacking faults or intergrowth,[24,26] although Zandbergen et al. report the observation of additional members of the above series for $n \neq 0$ (in particular, $Pb_2Sr_2Cu_2O_{6+\delta}$ and $Pb_2Sr_2(Y,Ca)_2Cu_4O_{10+\delta}$) present as single planar defects in a small fraction of their samples.[27] A representative high-resolution electron diffraction image for $Pb_2Sr_2MCu_3O_8$ is shown in Figure 6 with arrows indicating the Cu–O double layers.

In the case of the bismuth or thallium alkaline-earth metal cuprates, Ca^{2+} ions separate the infinite Cu–O sheets. However, in $Pb_2Sr_2(M,Ca)Cu_3O_8$ the Cu–O sheets are separated by M^{3+} ions or a mixture of M^{3+} and Ca^{2+} ions; addition of $CaCuO_2$ layers to this structure would result in loss of the local charge neutrality of the Cu–O sheets. Thus, frequent intergrowths are less likely in this system than in the BiSrCaCuO or TlBaCaCuO Aurivillius-related phases. A similar situation exists in $Ba_2YCu_3O_7$; while the chain portion of the structure can be replaced by double chains, no phases containing additional Cu–O planes have been prepared.

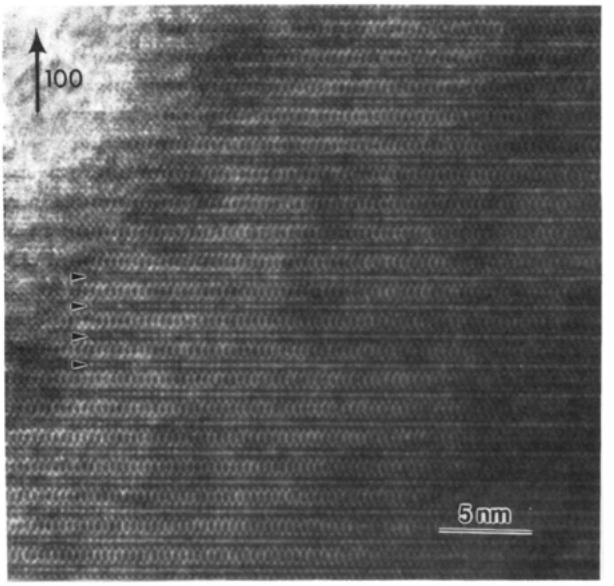

Figure 6. High-resolution electron micrograph of the [100] plane of $Pb_2Sr_2MCu_3O_8$.

Conclusions

Like $Ba_2YCu_3O_7$, the newly discovered family of cuprate superconductors represented by $Pb_2Sr_2YCu_3O_8$ has a rich substitutional chemistry. We have prepared $Pb_2Sr_2MCu_3O_8$ and $Pb_2Sr_2M_{1-x}AE_xCu_3O_{8+\delta}$ samples in both ceramic and single-crystal form for a variety of lanthanoids. The growth of single crystals from PbO fluxes is described and should allow further investigations of the physical properties of these interesting new materials. Systematic structural changes are observed as a function of lanthanoid size, with the larger lanthanoids enlarging the unit cell, particularly along the x axis. Upon being doped with an alkaline-earth metal ion on the lanthanoid site, the materials become bulk superconductors. In agreement with recent neutron and electron diffraction studies, single-crystal structural refinements provide additional evidence for shifts in the positions of the oxygens in the Pb–O planes to account for the observed orthorhombicity of the materials. Finally, we have reported the synthesis of a new compound of stoichiometry $Pb_2Ba_2YCu_3O_8$ in which the strontium has been replaced by barium.

Acknowledgment. We thank B. Batlogg, D. W. Murphy, and S. A. Sunshine for helpful discussions.

Supplementary Material Available: A listing of structure factor amplitudes (4 pages). Ordering information is given on any current masthead page.

(25) Zandbergen, H. W.; Groen, W. A.; van Tendeloo, G.; Amelinckx, S. *Appl. Phys. A* **1989**, *48*, 305.
(26) Hull, R.; Bonar, J. M.; Schneemeyer, L. F.; Cava, R. J.; Krajewski, J. J.; Waszczak, J. V. *Phys. Rev. B* **1989**, *39*, 9685.
(27) Zandbergen, H. W.; Kadowaki, K.; Menken, M. J. V.; Menovsky, A. A.; van Tendeloo, G.; Amelinckx, S., preprint.
(28) Shannon, R. D. *Acta Crystallogr.* **1976**, *A22*, 751.